Supplement of Hydrol. Earth Syst. Sci., 20, 3343–3359, 2016
http://www.hydrol-earth-syst-sci.net/20/3343/2016/
doi:10.5194/hess-20-3343-2016-supplement

Hydrology and Earth System Sciences
Open Access
EGU

Supplement of

Projected impacts of climate change on hydropower potential in China

Xingcai Liu et al.

Correspondence to: Qiuhong Tang (tangqh@igsnrr.ac.cn)

Tables

Table S1. Main characteristics of the GHMs used in this study, based on Schewe et al. (2014).

Model name	Time step length	Meteorological forcing *	Energy balance	Evaporation scheme	Runoff scheme	Snow scheme	Vegetation dynamics	CO_2 effect	References
DBH	1hr	P, T, W, Q, LW, SW, SP	Yes	Energy balance	Infiltration excess	Energy balance	No	Constant	Tang et al. (2007)
H08	Daily	R, S, T, W, Q, LW, SW, SP	Yes	Bulk formula	Saturation excess, non-linear	Energy balance	No	No	Hanasaki et al. (2008)
Mac-PDM.09	Daily	P, T, W, Q, LWn, SW	No	Penman-Monteith	Saturation excess, non-linear	Degree-day	No	No	Gosling and Arnell (2011)
MATSIRO	1hr	R, S, T, W, Q, LW, SW, SP	Yes	Bulk formula	Infiltration excess, saturation excess, groundwater.	Energy balance	No	Constant	Takata et al. (2003)
MPI-HM	Daily	P, T, W, Q, LWn, SW, SP	No	Penman-Monteith	Saturation excess, non-linear	Degree-day	No	No	Hagemann and Gates (2003)
PCR-GLOBWB	Daily	P, T	No	Hamon	Saturation Excess Beta Function	Degree Day	No	No	van Beek et al. (2011)
VIC	Daily, 3hr snow	P, T, W, Q, LW, SW, SP.	Only for snow.	Penman-Monteith	Saturation excess, non-linear	Energy balance.	No	No	Liang et al. (1994)
WBM	Daily	P, T	No	Hamon	Saturation Excess	Empirical formula	No	No	Wisser et al. (2010)

* P: precipitation, T: temperature, W: wind speed, Q: air specific humidity, LW: downwelling longwave, SW: downwelling shortwave, SP: surface pressure.

Table S2. GCMs used in this study.

GCM	Institution	Description
GFDL-ESM2M	Geophysical Fluid Dynamics Laboratory	Dunne, et al. (2012)
HadGEM2-ES	Met Office Hadley Centre, UK	Jones, et al. (2011)
IPSL-CM5A-LR	Institut Pierre-Simon Laplace Climate Modelling Centre	Dufresne et al. (2013)
MIROC-ESM-CHEM	Japan Agency for Marine-Earth Science and Technology, the Atmosphere and Ocean Research Institute at the University of Tokyo, and the National Institute for Environmental Studies	Watanabe, et al., (2011)
NorESM1-M	Norwegian Climate Centre	Bentsen et al. (2013)

Table S3. Sensitivity tests for parameters of DHP calculation (see Equation 1).

Parameter	**Values**
α	0.65, 0.75, **0.85**, 0.95
β	1, **2**, 3
K_c	0.4, **0.5**, 0.6
IHC	0.9*IHC, **IHC**, 1.1*IHC

The bold numbers are the values used in present study. 0.9*IHC means IHC decrease by 10%, 1.1*IHC means IHC increase by 10%.

Table S4. Percentiles of relative annual *GHP* changes (%) of China over 2020-2050 across GHMs and GCMs, respectively

Percentile / **GHM**	RCP2.6			RCP8.5		
	50th	25th	75th	50th	25th	75th
DBH	4.73	1.50	5.37	1.73	0.37	4.93
H08	4.13	1.03	5.00	0.91	-0.48	1.94
Mac-PDM.09	1.89	0.40	4.83	0.24	-2.97	1.12
MATSIRO	1.06	-4.43	2.34	-5.77	-7.44	19.82
MPI-HM	4.49	-2.08	5.02	-2.74	-3.81	-0.45
PCR-GLOBWB	4.17	2.35	4.76	1.36	-0.45	3.66
VIC	-1.38	-3.81	1.74	-3.95	-6.96	-2.15
WBM	-0.16	-3.90	2.93	-4.77	-8.03	-2.61
GCM						
GFDL-ESM2M	4.37	2.52	4.88	-0.97	-3.22	0.93
HadGEM2-ES	-5.20	-9.05	-1.80	-5.83	-9.79	-2.66
IPSL-CM5A-LR	4.89	3.28	5.75	2.66	-0.69	4.40
MIROC-ESM-CHEM	0.61	-2.13	3.20	0.87	-3.42	3.72
NorESM1-M	2.16	0.87	3.81	-1.75	-6.03	0.27
All	2.22	-1.21	4.58	-1.71	-4.36	1.41

Table S5. Percentiles of relative annual *GHP* changes (%) of China over 2070-2099 across GHMs and GCMs, respectively

Percentile / **GHM**	RCP2.6			RCP8.5		
	50th	25th	75th	50th	25th	75th
DBH	5.18	2.31	9.45	13.11	9.86	23.04
H08	4.25	0.62	6.22	7.03	5.80	10.58
Mac-PDM.09	3.65	1.37	5.12	5.97	1.66	13.00
MATSIRO	0.92	-3.90	326.27	-6.08	-7.35	19.02
MPI-HM	1.07	-2.32	5.81	4.84	2.90	11.50
PCR-GLOBWB	6.85	3.24	8.15	8.62	7.51	15.66
VIC	-2.10	-3.30	0.27	-5.31	-7.24	2.79
WBM	1.74	-0.69	4.82	-1.94	-7.11	4.57
GCM						
GFDL-ESM2M	-1.53	-4.09	-0.20	5.38	-0.55	7.81
HadGEM2-ES	2.80	-0.52	5.72	-1.34	-10.01	4.62
IPSL-CM5A-LR	1.50	-0.77	3.55	7.42	-0.88	12.29
MIROC-ESM-CHEM	8.86	6.71	10.03	20.63	13.99	26.56
NorESM1-M	4.44	2.28	5.27	3.51	-5.71	7.60
All	2.93	-0.53	6.71	6.27	-2.36	10.57

Table S6. Percentiles of relative seasonal *GHP* changes (%) of China over 2020-2050 (2035) and 2070-2099 (2085) across the ensemble of GCM-GHM combinations.

Percentile / **Season**	RCP2.6			RCP8.5		
	50th	25th	75th	50th	25th	75th
2035						
MAM	0.43	-2.29	2.39	-1.43	-5.87	0.75
JJA	0.38	-2.87	3.78	-2.31	-7.50	-0.60
SON	3.86	-0.17	8.14	1.68	-2.27	6.06
DJF	1.36	-3.98	7.73	-0.57	-3.53	5.63
2085						
MAM	-0.77	-5.54	2.36	-0.06	-9.78	6.84
JJA	1.49	-1.46	4.39	6.86	-4.48	14.13
SON	7.46	0.28	10.82	7.88	2.79	17.46
DJF	3.62	-3.88	11.35	2.51	-7.82	11.40

Table S7. Percentiles of relative annual *DHP* changes (%) of China over 2020-2050 across GHMs and GCMs, respectively

Percentile / GHM	RCP2.6			RCP8.5		
	50th	25th	75th	50th	25th	75th
DBH	0.32	-0.93	3.21	-1.30	-3.23	2.27
H08	-0.86	-5.04	0.89	-4.51	-7.61	-0.13
Mac-PDM.09	-0.42	-4.39	1.12	-5.41	-6.34	-1.08
MATSIRO	-2.70	-7.10	18.37	-7.65	-11.92	-4.02
MPI-HM	-2.86	-7.54	-0.93	-9.41	-10.82	-3.20
PCR-GLOBWB	-1.22	-4.23	0.96	-5.47	-6.07	-1.05
VIC	-4.99	-8.59	-1.90	-5.64	-8.75	-1.47
WBM	-4.43	-8.78	-1.69	-10.64	-12.83	-6.47
GCM						
GFDL-ESM2M	-2.41	-3.85	-1.04	-6.62	-10.03	-4.99
HadGEM2-ES	-0.29	-2.45	0.32	-1.37	-3.63	-0.63
IPSL-CM5A-LR	-4.36	-5.76	-2.32	-7.70	-11.32	-5.79
MIROC-ESM-CHEM	-6.66	-10.39	-3.18	-8.59	-11.22	-5.98
NorESM1-M	2.80	1.63	3.19	-1.28	-3.27	-0.08
All	-2.22	-4.91	0.33	-5.44	-8.95	-1.46

Table S8. Percentiles of relative annual *DHP* changes (%) of China over 2070-2099 across GHMs and GCMs, respectively

Percentile / **GHM**	RCP2.6			RCP8.5		
	50th	25th	75th	50th	25th	75th
DBH	3.72	-1.50	5.57	7.51	-1.34	8.04
H08	-0.98	-5.06	2.23	-2.82	-9.83	0.05
Mac-PDM.09	1.93	-3.50	3.25	-0.91	-7.35	2.14
MATSIRO	-1.19	-5.97	16.13	-8.78	-20.93	8.77
MPI-HM	-1.33	-8.58	0.20	-4.45	-15.09	-3.47
PCR-GLOBWB	2.63	-3.49	4.63	1.16	-8.39	1.88
VIC	-5.60	-9.70	-1.11	-4.35	-12.41	-2.96
WBM	1.49	-6.66	3.98	-6.26	-16.74	-4.81
GCM						
GFDL-ESM2M	-5.11	-7.03	-2.53	-9.24	-13.67	-5.16
HadGEM2-ES	3.44	0.70	6.13	0.17	-2.56	2.12
IPSL-CM5A-LR	-5.75	-8.44	-2.61	-16.75	-22.63	-11.77
MIROC-ESM-CHEM	-1.15	-2.59	2.06	-3.22	-4.67	4.33
NorESM1-M	2.50	-0.52	3.70	-2.63	-5.36	0.69
All	-1.08	-4.87	2.71	-3.68	-10.23	0.38

Reference

Bentsen, M., et al., 2013: The Norwegian Earth System Model, NorESM1-M – Part 1: Description and basic evaluation of the physical climate. Geosci. Model Dev., 6 (3), 687-720.
Dufresne, J. L., et al., 2013: Climate change projections using the IPSL-CM5 Earth System Model: from CMIP3 to CMIP5. Clim. Dyn., 40 (9-10), 2123-2165.
Gosling, S. N., and N. W. Arnell, 2011: Simulating current global river runoff with a global hydrological model: model revisions, validation, and sensitivity analysis. Hydrol. Processes, 25 (7), 1129-1145.
Hagemann, S., and L. D. Gates, 2003: Improving a subgrid runoff parameterization scheme for climate models by the use of high resolution data derived from satellite observations. Clim. Dyn., 21 (3-4), 349-359.
Hanasaki, N., S. Kanae, T. Oki, K. Masuda, K. Motoya, N. Shirakawa, Y. Shen, and K. Tanaka, 2008: An integrated model for the assessment of global water resources – Part 1: Model description and input meteorological forcing. Hydrol. Earth Syst. Sci., 12 (4), 1007-1025.
Dunne, John P., et al., 2012: GFDL's ESM2 Global Coupled Climate–Carbon Earth System Models. Part I: Physical Formulation and Baseline Simulation Characteristics. J. Climate, 25, 6646–6665. doi: 10.1175/JCLI-D-11-00560.1.
Jones, C. D., et al., 2011: The HadGEM2-ES implementation of CMIP5 centennial simulations. Geosci. Model Dev., 4 (3), 543-570.
Liang, X., D. P. Lettenmaier, E. F. Wood, and S. J. Burges, 1994: A simple hydrologically based model of land surface water and energy fluxes for general circulation models. J. Geophys. Res., 99 (D7), 14415-14428.
Schewe, J., et al., 2014: Multimodel assessment of water scarcity under climate change. Proc. Nat. Acad. Sci. U.S.A., 111, 3245-3250.
Takata, K., S. Emori, and T. Watanabe, 2003: Development of the minimal advanced treatments of surface interaction and runoff. Global Planet. Change, 38 (1–2), 209-222.
Tang, Q., T. Oki, S. Kanae, and H. Hu, 2007: The influence of precipitation variability and partial irrigation within grid cells on a hydrological simulation. J. Hydrometeor, 8, 499-512.
van Beek, L. P. H., Y. Wada, and M. F. P. Bierkens, 2011: Global monthly water stress: 1. Water balance and water availability. Water Resour. Res., 47 (7), W07517.
Watanabe, S., et al., 2011: MIROC-ESM 2010: model description and basic results of CMIP5-20c3m experiments. Geosci. Model Dev., 4 (4), 845-872.
Wisser, D., B. M. Fekete, C. J. Vörösmarty, A. H. Schumann, 2010: Reconstructing 20th century global hydrography: a contribution to the Global Terrestrial Network- Hydrology (GTN-H). Hydrol. Earth Syst. Sci., 14 (1), 1-24.

Figures

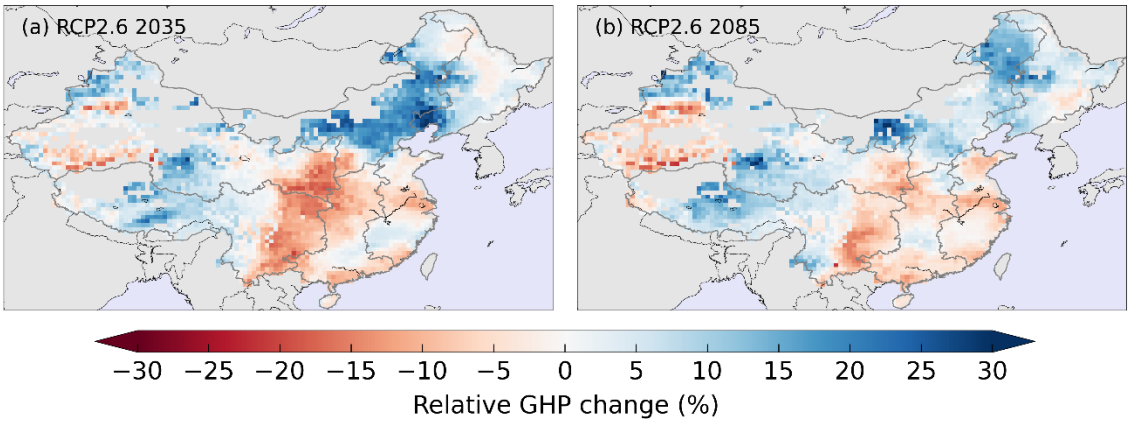

Figure S1. Medians of relative changes in the annual mean GHPs for 2020-2050 (a) and 2070-2099 (b) compared to the historical period (1971-2000) across the ensemble of GCM-GHM combinations under RCP2.6.

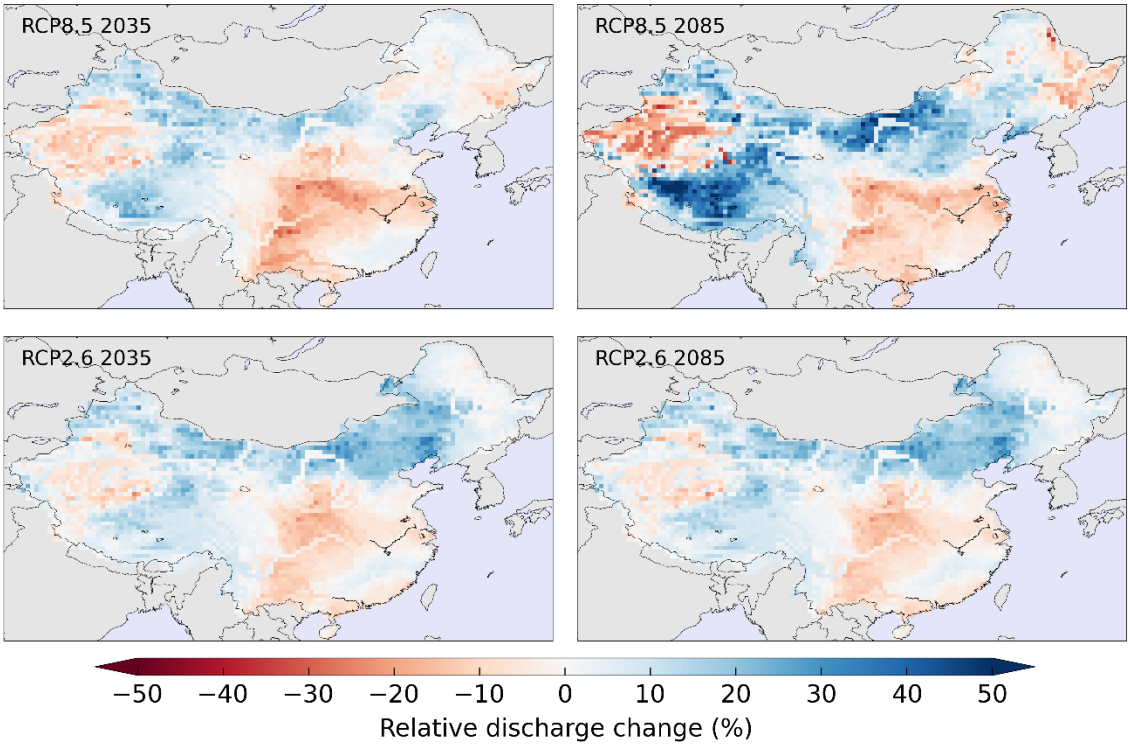

Figure S2. Medians of relative changes in annual discharge (without regulation) across the ensemble of GCM-GHM combinations for 2020-2050 (2035) and 2070-2099 (2085) compared to the historical period (1971-2000).

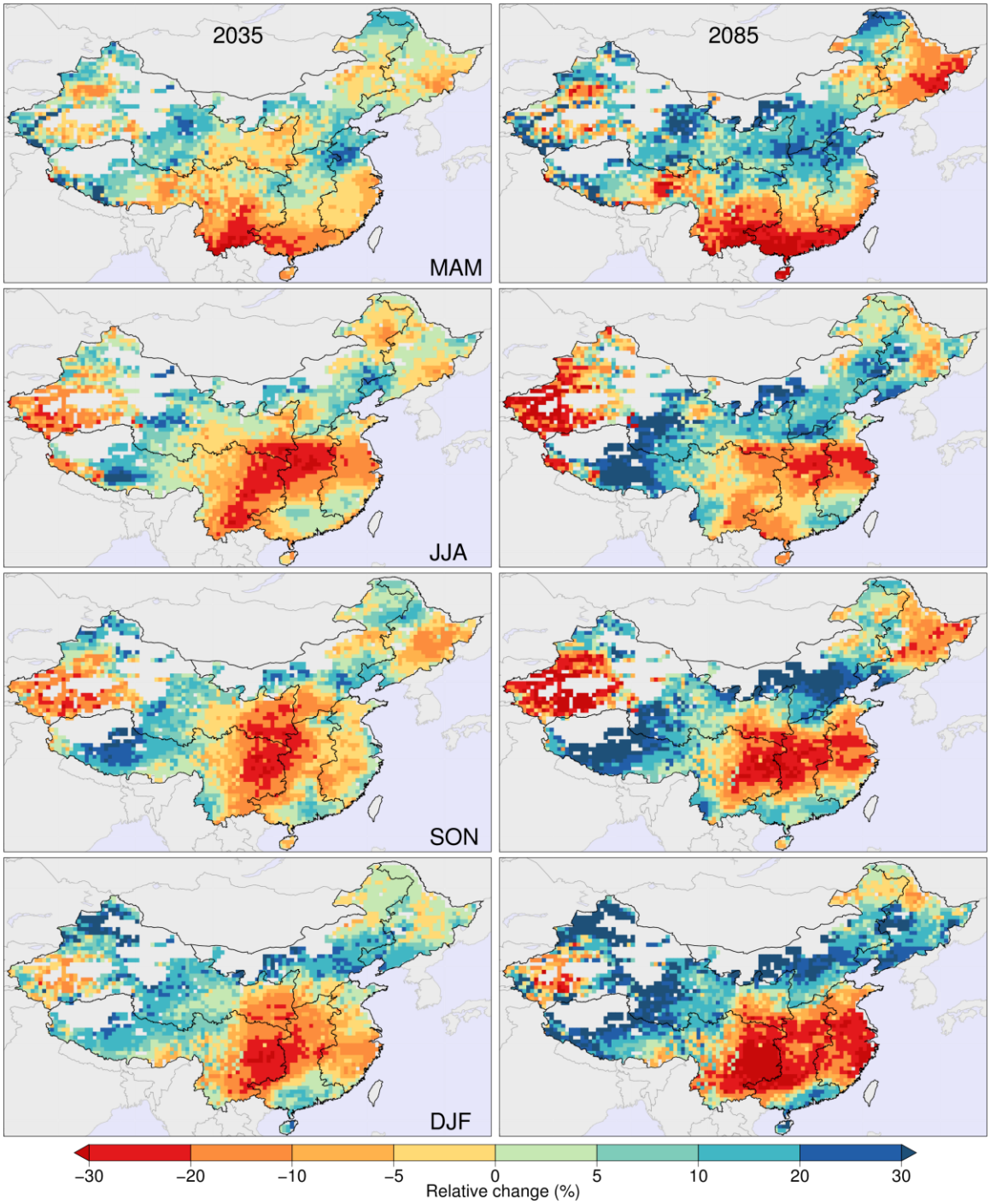

Figure S3. Medians of relative seasonal GHP changes for 2020-2050 (left) and 2070-2099 (right) under RCP8.5.

MAM: March, April, May; JJA: June, July, August; SON: September, October, November; DJF: December, January, February.

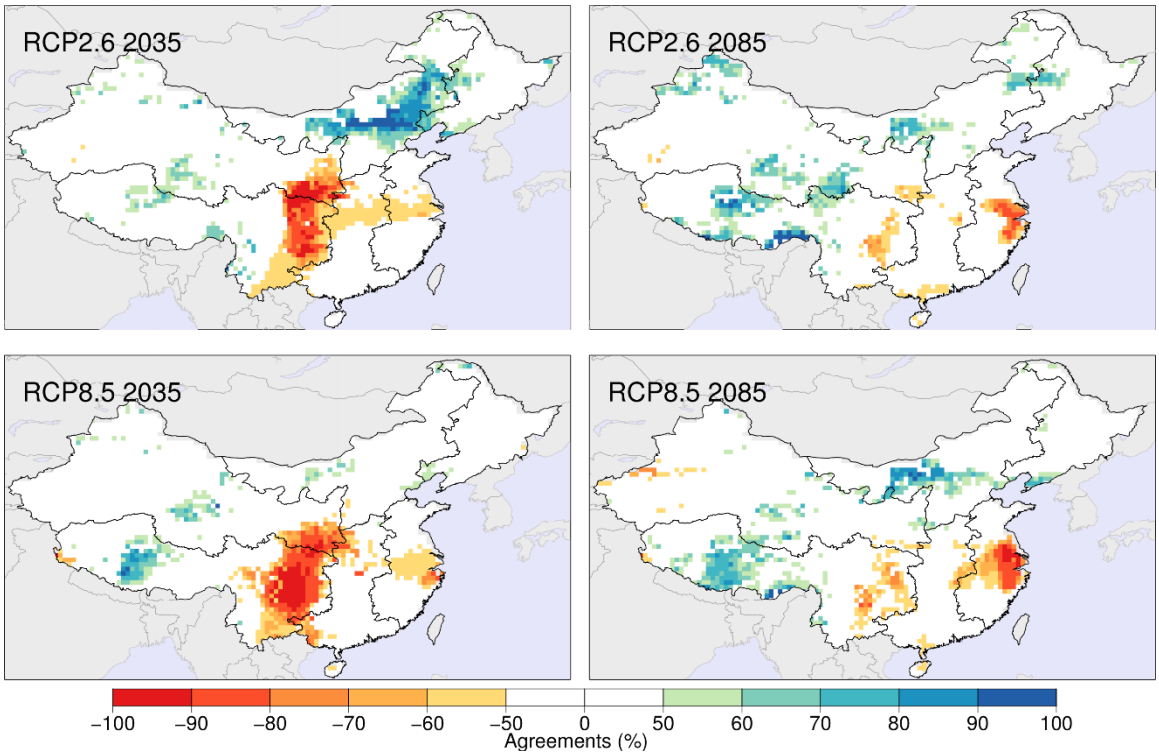

Figure S4. Agreements between relative GHP changes across the ensemble of GCM-GHM combinations calculated as the difference of positive and negative fractions of total ensemble.

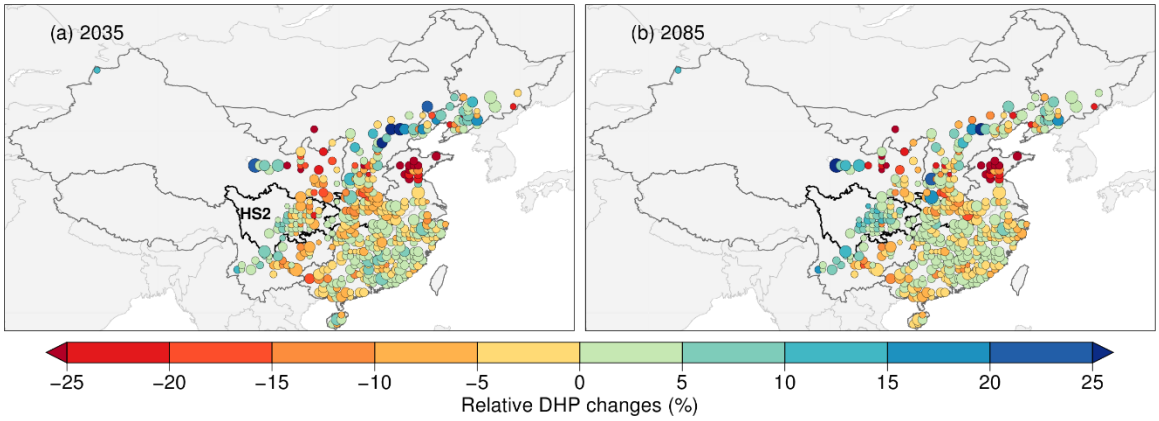

Figure S5. Relative DHP changes for each reservoir for 2020-2050 (2035) and 2070-2099 (2085) under RCP2.6.

Black line depicts the hotspot region HS2, i.e. Sichuan (including Chongqing) and Hubei provinces. Circle size is determined according to the logarithm of reservoir storage capacity.

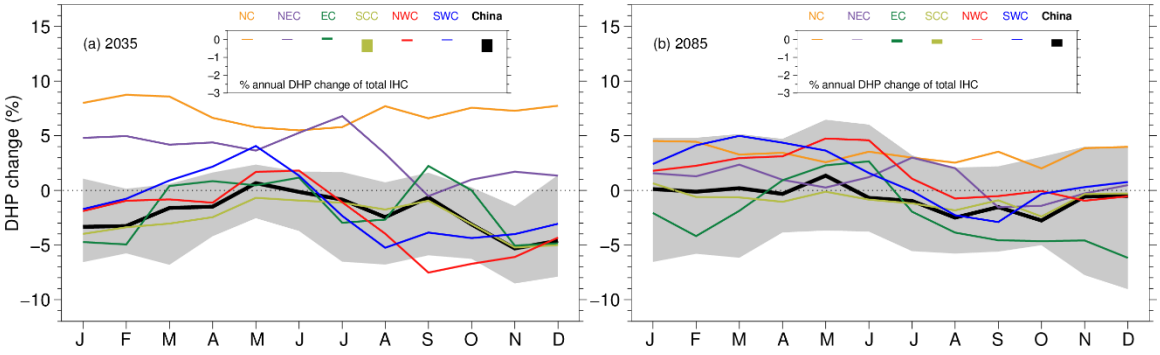

Figure S6. Relative DHP changes for regions of China for 2020-2050 (2035) and 2070-2099 (2085) under RCP2.6.

Lines show the ensemble medians across all GCM-GHM combinations; grey areas show the IQR of relative DHP changes of China; the inner plots show annual DHP changes of regions in terms of percentage of IHC.

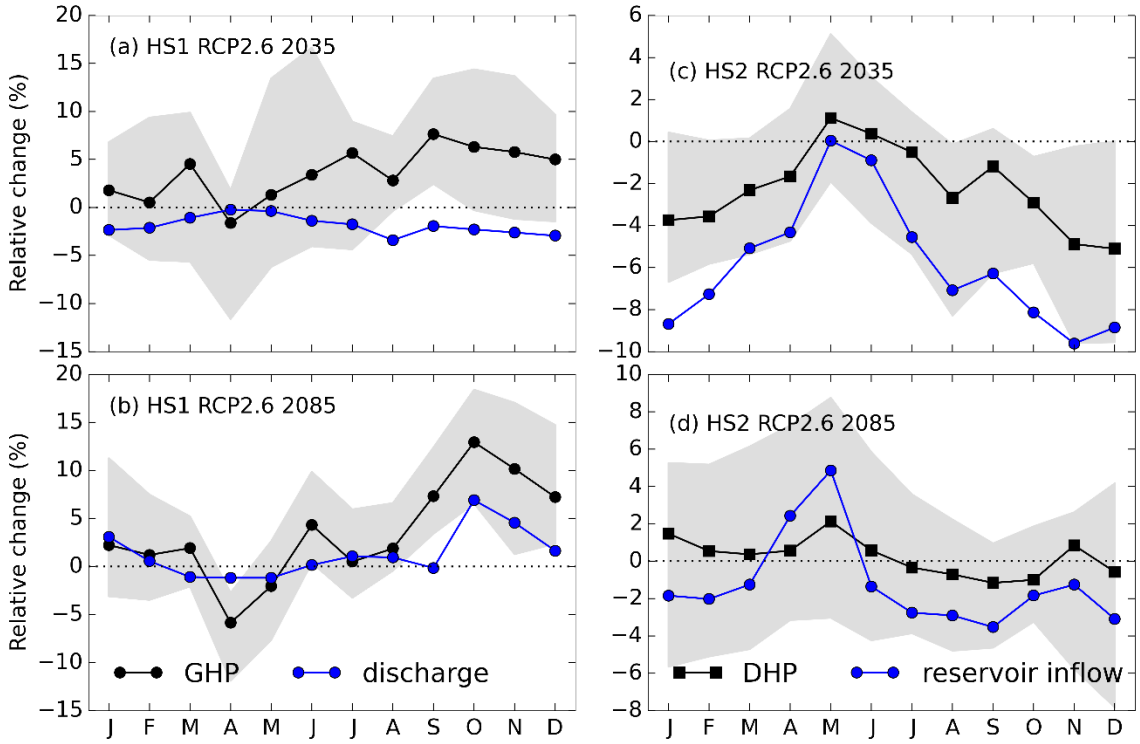

Figure S7. Relative changes in monthly GHPs (DHPs) and discharges (reservoir inflow) for hotspot regions for 2020-2050 (2035) and 2070-2099 (2085) under RCP2.6.

HS1: the hotspot region in Southwest China (see Figure 2); HS2: Sichuan and Hubei provinces (see Figure 6). Lines denote the ensemble medians across all GCM-GHM combinations and grey areas denote the IQRs across the ensemble of GCM-GHM combinations.

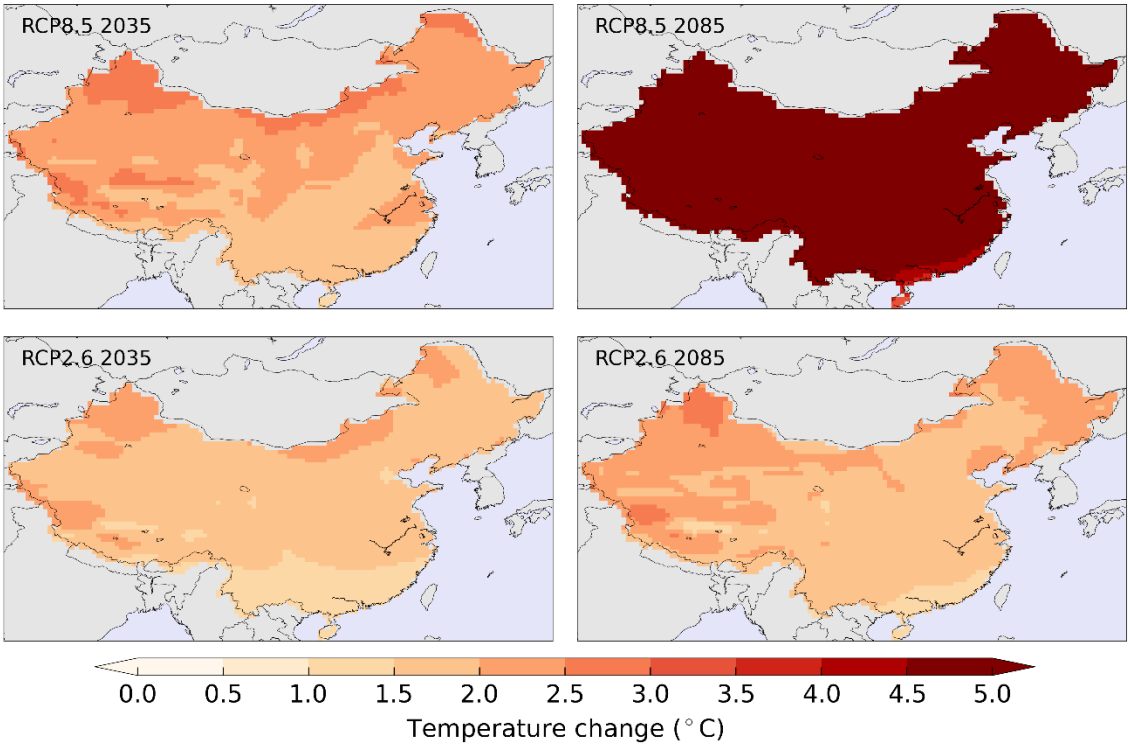

Figure S8. Medians of annual mean temperature changes in China in 2035 and 2085 compared to the historical period (1971-2000) across the five GCMs.

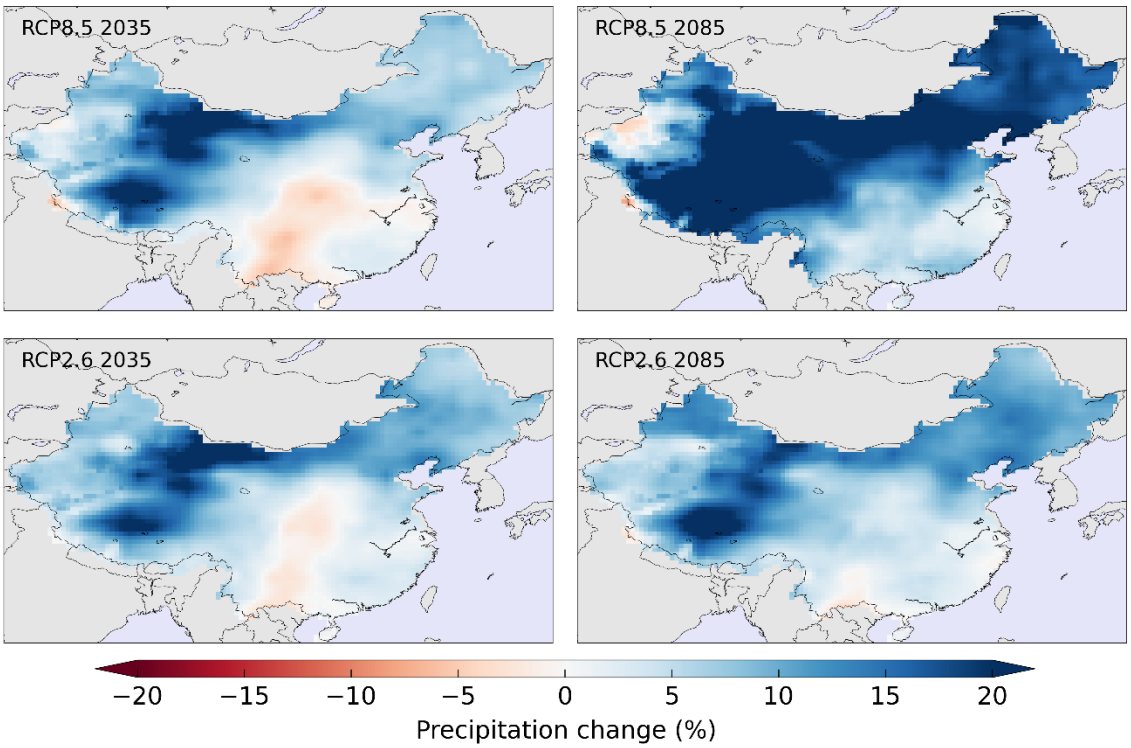

Figure S9. Medians of relative annual precipitation changes in China in 2035 and 2085 compared to the historical period (1971-2000) across the five GCMs.

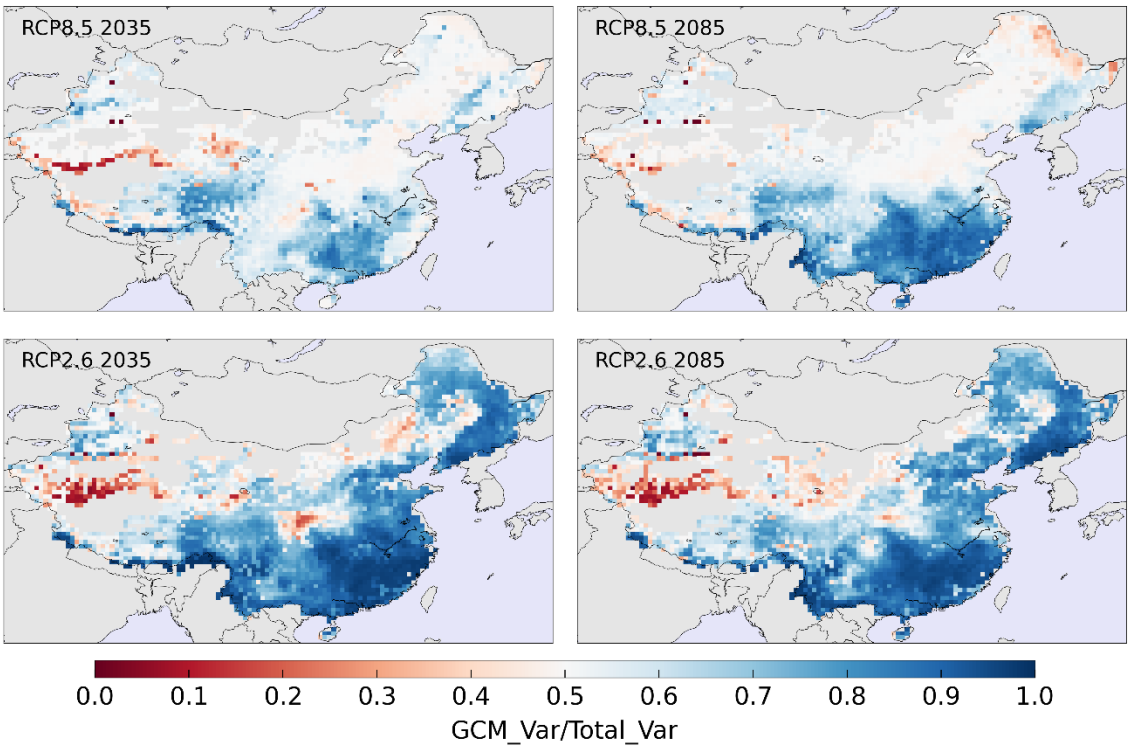

Figure S10. The ratio of GCM variance to total variance across all GCMs and GHMs.

GCM variance is computed across all GCMs for each GHM individually and then averaged over all GHMs, vice versa for GHM variance. In blue (red) areas, GCM (GHM) variance predominates.

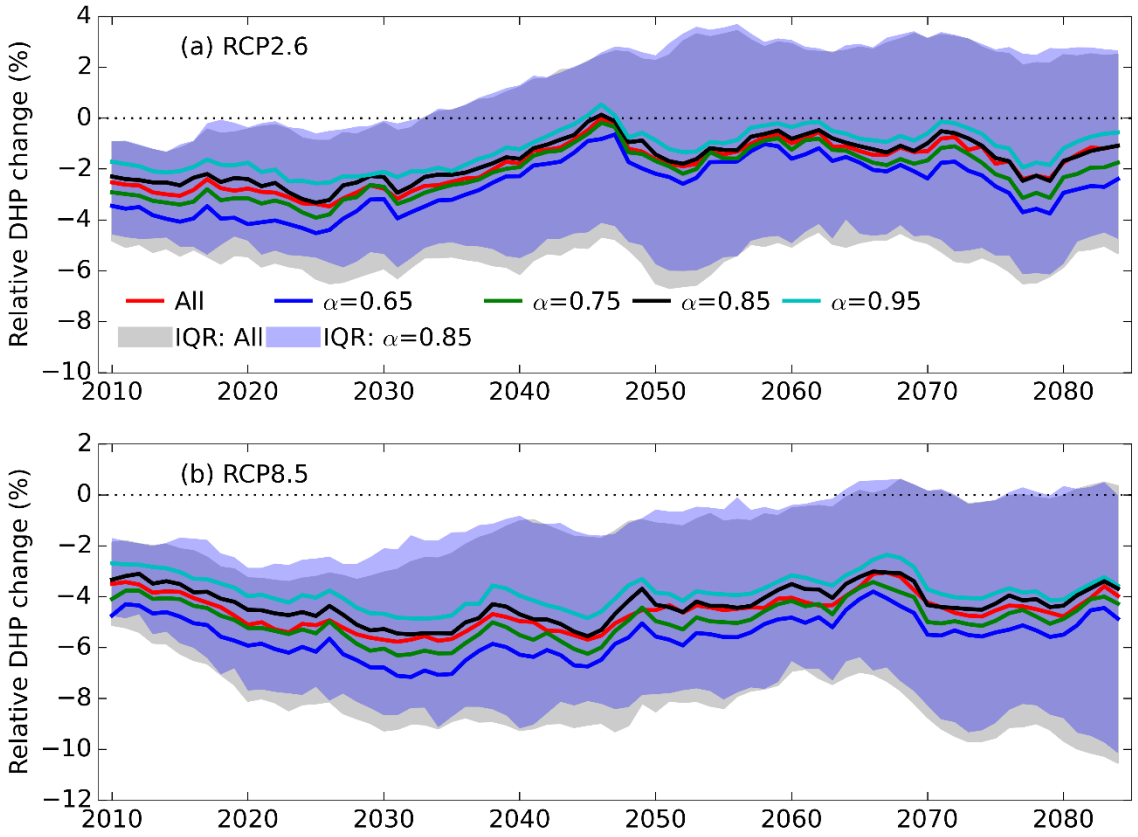

Figure S11. Medians of relative changes in the DHPs of present reservoirs in China over the 2010-2084 period under RCP2.6 (a) and RCP8.5 (b) for different α values.

To test the sensitivity of DHP to α values, several experiments with different α (=0.65, 0.75, 0.85, 0.95) are carried out. Color lines show the medians of DHP for different α values. The black line shows the DHP in present study with α=0.85. The gray area shows the range of 25th and 75th from the ensemble of GCM-GHM combinations for all α values, while the light blue area shows the range of 25th and 75th from the ensemble of GCM-GHM combinations for α=0.85.

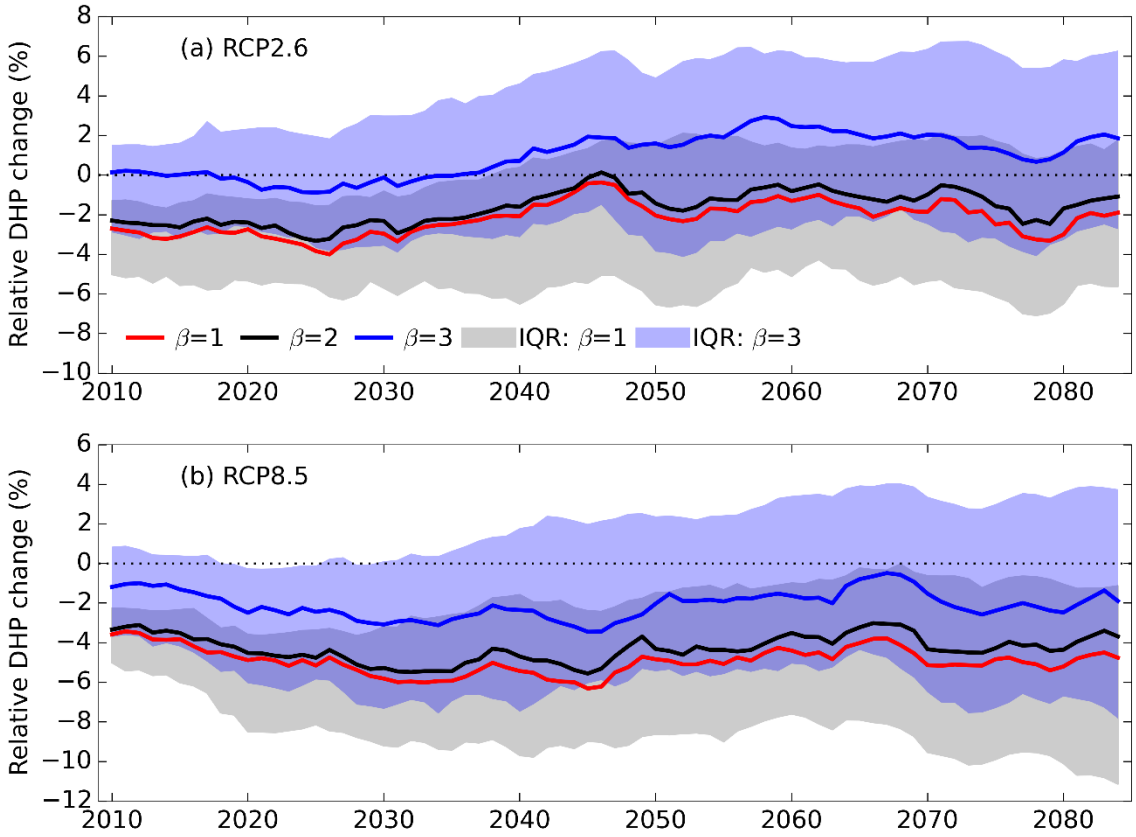

Figure S12. Medians of relative changes in the DHPs of present reservoirs in China over the 2010-2084 period under RCP2.6 (a) and RCP8.5 (b) for different β values.

Two experiments with different exponents of (c/K_c) β (see Equation 1) are carried out. Color lines show the medians of DHP for different β values. The black line shows the DHP in present study with $\beta = 2$ (used in this study). The gray area shows the range of 25th and 75th from the ensemble of GCM-GHM combinations for $\beta = 1$, while the light blue area shows the range of 25th and 75th from the ensemble of GCM-GHM combinations for $\beta = 2$.

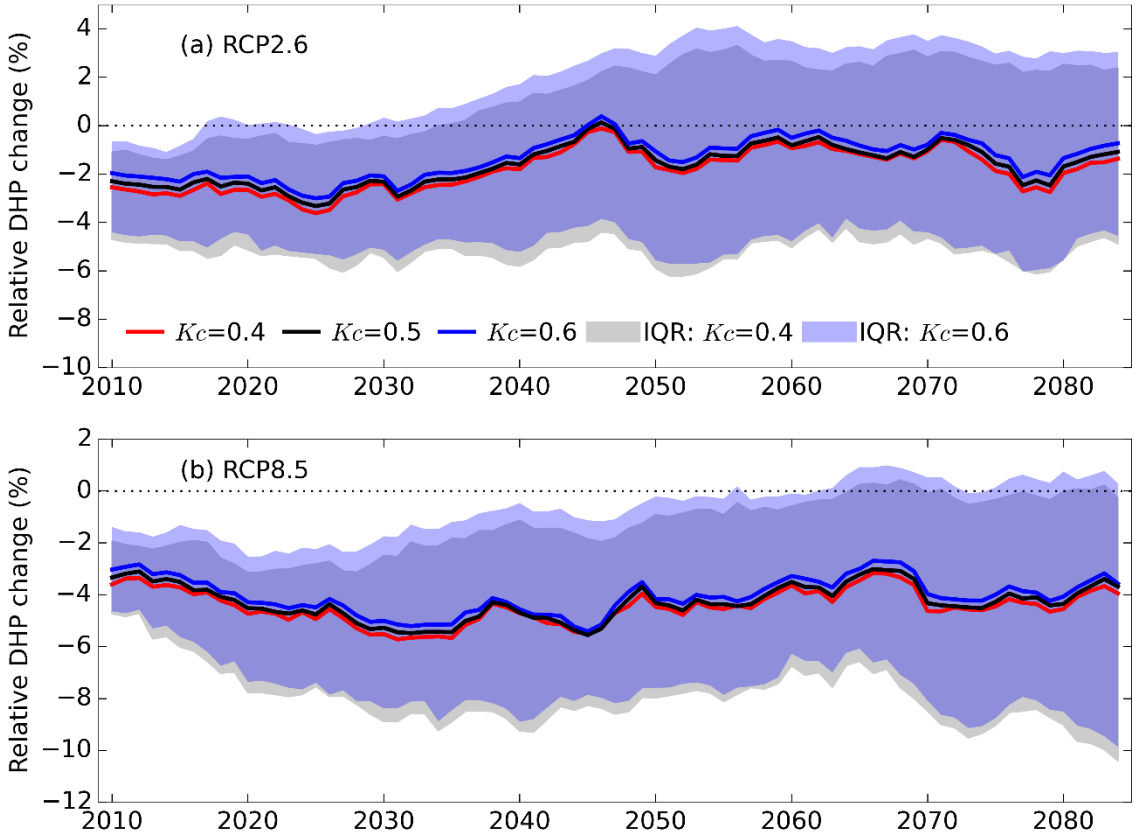

Figure S13. Medians of relative changes in the DHPs of present reservoirs in China over the 2010-2084 period under RCP2.6 (a) and RCP8.5 (b) for different K_c values.

Two experiments with different *c* criterions (K_c, see Equation 1) are carried out. Color lines show the medians of DHP for different criterions. The black line shows the DHP in present study with K_c = 0.5 (used in this study). The gray area shows the range of 25th and 75th from the ensemble of GCM-GHM combinations for K_c = 0.4, while the light blue area shows the range of 25th and 75th from the ensemble of GCM-GHM combinations for K_c = 0.6.

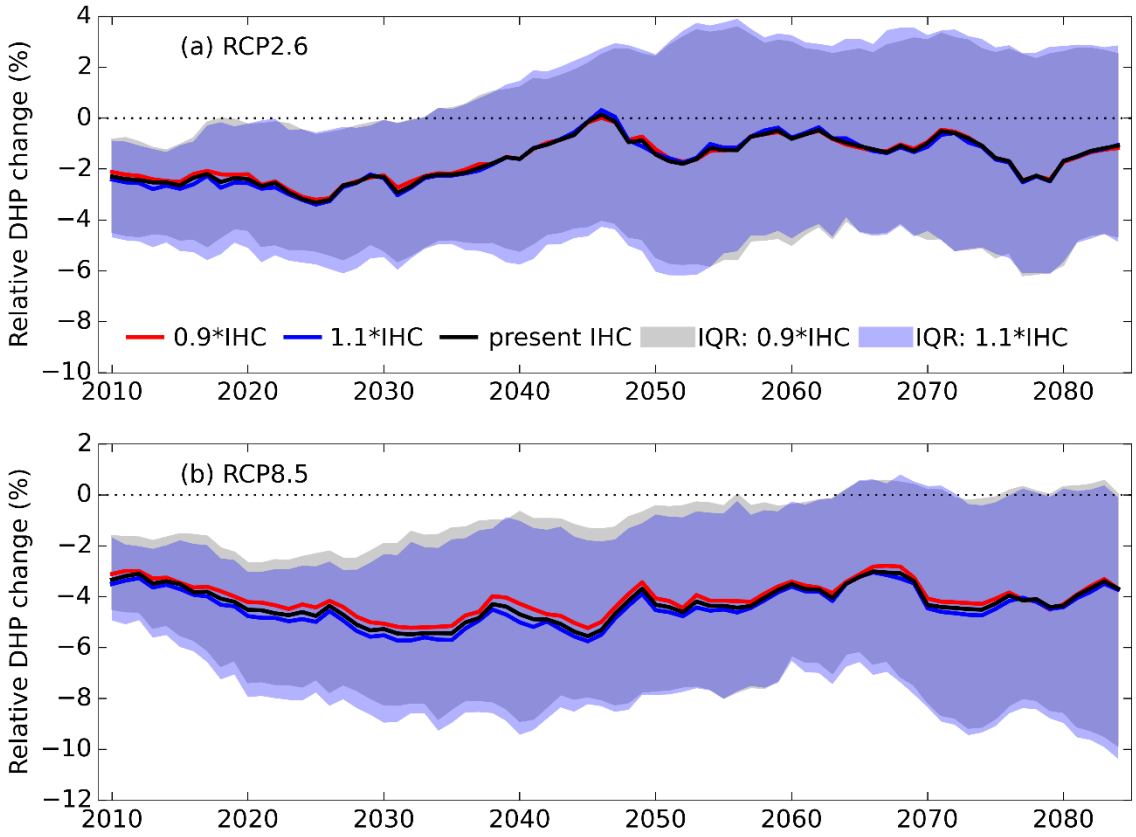

Figure S14. Medians of relative changes in the DHPs of present reservoirs in China over the 2010-2084 period under RCP2.6 (a) and RCP8.5 (b) for different IHCs.

To test the sensitivity of DHP to the IHC data, two experiments with IHC decrease by 10% (0.9*IHC) and increase by 10% (1.1*IHC), respectively, are carried out. Color lines show the medians of DHP for different IHC. The black line shows the DHP in present study with present IHC. The gray area shows the range of 25th and 75th from the ensemble of GCM-GHM combinations for 0.9*IHC, while the light blue area shows the range of 25th and 75th from the ensemble of GCM-GHM combinations for 1.1*IHC.